TECHNICAL REPORT

For the

EARTH PHYSICS PROGRAM

OFFICE OF NAVAL RESEARCH
Contract # N00014-75-C-1126

ACOUSTIC PROPERTIES OF SHELVES: SOUTH ATLANTIC MARGINS

by

Robert E. Houtz

Lamont-Doherty Geological Observatory of Columbia University
Palisades, New York 10964

L-DGO # CU-1-78

Technical Report #1

UNCLASSIFIED
SECURITY CLASSIFICATION OF THIS PAGE (When Data Entered)

REPORT DOCUMENTATION PAGE		READ INSTRUCTIONS BEFORE COMPLETING FORM
1. REPORT NUMBER L-DGO CU-178	2. GOVT ACCESSION NO.	3. RECIPIENT'S CATALOG NUMBER
4. TITLE (and Subtitle) Acoustic Properties of Shelves: South Atlantic Margins		5. TYPE OF REPORT & PERIOD COVERED Research 1968-1978
		6. PERFORMING ORG. REPORT NUMBER
7. AUTHOR(s) Robert E. Houtz		8. CONTRACT OR GRANT NUMBER(s) N00014-75-C-1126
9. PERFORMING ORGANIZATION NAME AND ADDRESS Lamont-Doherty Geological Observatory Palisades, New York 10964		10. PROGRAM ELEMENT, PROJECT, TASK AREA & WORK UNIT NUMBERS
11. CONTROLLING OFFICE NAME AND ADDRESS Earth Physics Program Office of Naval Research, Washington, D.C.		12. REPORT DATE 11/24/78
		13. NUMBER OF PAGES 24
14. MONITORING AGENCY NAME & ADDRESS (if different from Controlling Office)		15. SECURITY CLASS. (of this report) Unclassified
		15a. DECLASSIFICATION/DOWNGRADING SCHEDULE

16. DISTRIBUTION STATEMENT (of this Report)

Approved for public release; distribution unlimited

17. DISTRIBUTION STATEMENT (of the abstract entered in Block 20, if different from Report)

18. SUPPLEMENTARY NOTES

19. KEY WORDS (Continue on reverse side if necessary and identify by block number)

20. ABSTRACT (Continue on reverse side if necessary and identify by block number)

DD FORM 1 JAN 73 1473 EDITION OF 1 NOV 65 IS OBSOLETE
S/N 0102-LF-014-6601

Unclassified
SECURITY CLASSIFICATION OF THIS PAGE (When Data Entered)

ACOUSTIC PROPERTIES OF SHELVES: SOUTH ATLANTIC MARGINS

By R.E. Houtz

Introduction

Acoustic information has been compiled from 5 regions of the South Atlantic as part of our continuing program of shelf studies. Results from each region are presented in a set of 3 maps, comprising the 15 maps shown as Figures 1a, 1b, and 1c through Figures 5a, 5b, and 5c. The first map in each regional series shows the locations of sonobuoys that were used to compile the velocity information, and the outlines of regions where velocity functions have been computed. The velocity functions are tabulated in Table 1 and keyed to the regions with a circled letter in the figures. The second map of the series shows approximate sediment isopachs contoured in units of kilometers. The third map shows approximate seafloor sound velocities contoured in km/sec. Wherever possible, previously published material was used.

Computation Methods

Owing to the poor acoustic penetration that is normally achieved with single-channel reflection profiling on shelves, sediment isopachs in this work have been based largely on sonobuoy solutions. These solutions are obtained either by use of critical refraction data or variable-angle reflection data. Both kinds of solution are based on the assumption of constant layer velocities, and are therefore directly comparable at the mid-points of the layers. This is borne out by statistical studies that show no significant difference between the two methods when the refraction velocity is taken as being in the middle of the layer. In some areas the reflection profiling provided reflection times to igneous basement. These times were converted to thickness by use of the appropriate velocity functions in Table 1.

In thick accumulations of sediment (>5 km), the basal sediment sound velocity may be indistinguishable from that of igneous basement. If the sediment thickness is variable, basement velocities can be identified by their independence of depth, as shown by Bryan and Simpson's (1971) sonobuoy data from the Orange Basin. In addition, basement roughness can introduce perturbations in the refraction data that are not usually present in refractions from sediment. However, in some areas basement has been arbitrarily defined as a horizon whose refraction velocity is greater than 5 km/sec. Along the northern margin of Brazil, the deepest consistent refraction velocity is 4.5 km/sec, and this number is used as the basis for a conservative estimate of total sediment thickness.

Seafloor sound velocities were determined principally from critical refractions that were observed at or slightly below seafloor. A significant portion (∿10% ?) yielded refraction lines that were .10 sec or more below seafloor; hence the seafloor sound velocity in these cases is not measurable with critical refractions. In a few cases the best estimate of seafloor sound velocity was obtained from interval velocity solutions (based on variable angle reflection data), but most of the measurements obtained when critical refractions were not available, were based on estimates of the critical angle of reflection. This method is outlined by Houtz (in press), who shows that the group velocity formed by the trailing edge of seafloor reflections is well-observed in many sonobuoy records. The seafloor velocity is computed simply by dividing the square of the water velocity by the group velocity.

Shelf sediments are sometimes too thin to develop velocity functions, and these areas are not included in the regional velocity functions tabulated in Table 1. For the most part, sediment velocity in sediments thinner than about 1 km can be estimated by using seafloor velocities. In a few other areas, discussed below, the results are too scattered to be useful; this has come about chiefly as the result of unusually rough subbottom topography.

Practically all the sonobuoy measurements were recorded with a passband between 5,and 40 Hz, in order to capitalize on the dominant bubble-pulse frequency of 18 Hz generated by the airguns.

South African Margin

Velocity functions were developed for the thick sediments of the Orange and the Outeniqua Basins. Functions obtained by Bryan and Simpson (1971) in the Orange Basin were based on refraction velocities that had not been corrected to the mid-points of the layers. The statistical information they derived is not suited for converting reflection times to thicknesses. Consequently it was necessary to re-pick all the Orange River sonobuoys to develop a useful velocity-depth function. The tabulated solutions of Leyden et al (1971) were used verbatim to develop the Outeniqua Basin velocity function.

The isopach map in the Orange Basin was compiled mainly from the work of Bryan and Simpson. Additional data was obtained from Rabinowitz (1976.) Results from Leyden et al were used to contour the Outeniqua Basin, which were modified in the eastern part of the basin with several unpublished sonobuoys and the 2-ship refraction results of Ludwig et al (1968). The general outline to the Agulhas arch was taken from Seisser et al (1974). The contouring from just north of Capetown to the southern edge of Agulhas shelf is comprised of unpublished sonobuoy data and from Leyden et al. No previous isopach contours have been made from the South African margin. The bathymetry of this margin is from Uchupi and Emery (1972).

Argentine Margin

The velocity functions in this study area (Figs. 2 and 3) were taken without modification from Houtz (1977), and the isopachs were traced without modification from Ludwig et al (1976). First layer velocities from Ludwig et al were used occasionally for seafloor velocities but most of them were determined by re-picking the original records. The critical reflection method was used extensively in the area west of the Falklands where the sediments are thin and the first refraction line is generally recorded below the seafloor. The very thick sediments to the south of this area provided a velocity function (Area C) but the velocity data from relatively thick sediments bounding area C yielded very scattered results and could not be used (standard error of estimate=500 m/sec). Except for the Rio Colorado Basin (Area D), the balance of the Argentine shelf is covered by sediments that are too thin to provide reliable velocity-depth data. No measurements are available in the San Jorge Basin at latitude 46°S on the Argentine coast. Note that a large number of 2-ship refraction solutions are available from the Argentine Margin. These solutions were used to estimate sediment thickness, but not the seafloor sound velocity.

Brazil Margin

This study area is shown in Figures 4 and 5. The velocity functions are taken from Houtz (op. cit.). The region east of area F yields very scattered results due to the widespread intrusion of salt diapirs. The isopachs were traced from Kumar et al (in press) with some modifications to the contours near the mouth of the Amazon River, based on the sonobuoy results of Houtz et al (1977). The isopach contours in Figure 5 B are based on the depth to a layer with a refraction velocity of about 4.5 km/sec, which is the deepest consistent refraction event that is measured in this area. However, it may not be igneous basement, and the contours therefore represent a conservative estimate of total sediment thickness.

Discussion

The seafloor sound velocity determined from the observation of critical reflections seems to give somewhat lower values than the observation of critical refractions. This discrepancy has not been studied in detail, although if it is real, more study would be appropriate. The discrepancy (based on only 8 comparisons) is in the expected direction, because thin layers of unconsolidated sediment lying atop high-speed refracting materials can be too thin to delay the head wave arrivals enough to be observable. On the other hand, the thin cover may be reflective. Hence the least-time path of head waves will sample the high-speed materials and their refraction line will appear to be tangent to the seafloor reflection curve.

A comparison of the seafloor sound velocity maps and the isopach maps reveal a tendency for thick sediment bodies to produce lower seafloor sound velocities. This seems to be related to the de-watering of slowly accumulating sediments, a process that lowers porosity and increases sound velocity. De-watering is hindered if additional overburden accumulates and blocks the outward flow of water.

References

Bryan, G., and E. Simpson, Seismic refraction measurements on the continental shelf between the Orange River and Cape Town, in The Geology of the East Atlantic Continental Margin, edited by F. Delaney, Institute of Geological Sciences Report No. 70/16, 187-198, 1971.

Houtz, R., Preliminary sonobuoy study of rapidly accumulating shelf sediments, J. Geophys. Res. (in press).

Houtz, R., Sound-velocity characteristics of sediment from the eastern South American margin, Geol. Soc. Am. Bull., 88, 720-722, 1977.

Houtz, R., W. Ludwig, J. Milliman, and J. Grow, Structure of the northern Brazilian continental margin, Geol. Soc. Am. Bull., 88, 711-719, 1977.

Leyden, R., M. Ewing and E. Simpson, Geophysical reconnaissance on African Shelf: 1 Cape Town to East London, Am. Assoc. Petroleum Geologists Bull., 55(5), 651-657, 1971.

Ludwig, W., G. Carpenter, R. Houtz, A Lonardi, and F. Rios, Sediment isopach map Argentine continental margin, Am. Assoc. Petroleum Geologists, Tulsa, Oklahoma, 1978.

Ludwig, W., J. Nafe, E. Simpson, and S. Sacks, Seismic-Refraction measurements on the southeast African continental margin, J. Geophys. Res., 73, 3707-3719, 1968.

Rabinowitz, P., Geophysical study of the continental margin of southern Africa, Geol. Soc. Am. Bull., 87, 1643-1653, 1976.

Seisser, W., R. Scrutton, and E. Simpson, Atlantic and Indian Ocean margins of southern Africa, in Continental Margins, edited by C. Burk and C. Drake, Springer-Verlag, 1974.

TABLE 1

$$V = V_o + K\,t \text{ (km/s)}$$

Area (See Figures)

	V_o	K	no. of points	Std. dev. Velocity	Correlation Coefficient
A	1.57	2.64	53	.24	.96
B	1.73	2.73	27	.19	.98
C	1.48	1.41	87	.26	.88
D	1.51	2.18	81	.19	.95
E	1.49	1.21	95	.20	.92
F	1.60	1.93	83	.26	.92
G	2.57	1.54	29	.27	.68
H	1.39	2.34	36	.22	.96

V_o = velocity at t = 0

K = regression coefficient (km/sec^2)

t = one-way vertical travel time

FIGURE CAPTIONS

1. South African Margin

   a. Sonobuoy locations and statistically studied sound velocity regions (letters coded in Table 1).

   b. Sediment isopach map contoured in km. Hatching indicates areas with less than 100 m of sediment.

   c. Seafloor sound velocity in km/s. Hatching indicates areas where velocity is $>$ 5 km/s.

2. Southern Argentine margin

   a. Sonobuoy locations and statistically studied sound velocity regions (letters coded in Table 1).

   b. Sediment isopach map contoured in km. Hatching indicates areas with less than 100 m of sediment.

   c. Seafloor sound velocity in km/s. Hatching indicates areas where velocity is $>$ 5 km/s.

3. Northern Argentine margin

   a. Sonobuoy locations and statistically studied sound velocity regions (letters coded in Table 1).

   b. Sediment isopach map contoured in km. Hatching indicates areas with less than 100 m of sediment.

   c. Seafloor sound velocity in km/s. Hatching indicates areas where velocity is $>$ 5 km/s.

4. Southern Brazilian margin.

   a. Sonobuoy locations and statistically studied sound velocity regions (letters coded in Table 1).

   b. Sediment isopach map contoured in km. Hatching indicates areas with less than 100 m of sediment.

   c. Seafloor sound velocity in km/s. Hatching indicates areas where velocity is > 5 km/s.

5. Northern Brazilian margin

   a. Sonobuoy locations and statistically studied sound velocity regions (letters coded in Table 1).

   b. Sediment isopach map contoured in km. Hatching indicates areas with less than 100 m of sediment.

   c. Seafloor sound velocity in km/s. Hatching indicates areas where velocity is > 4.5 km/s.

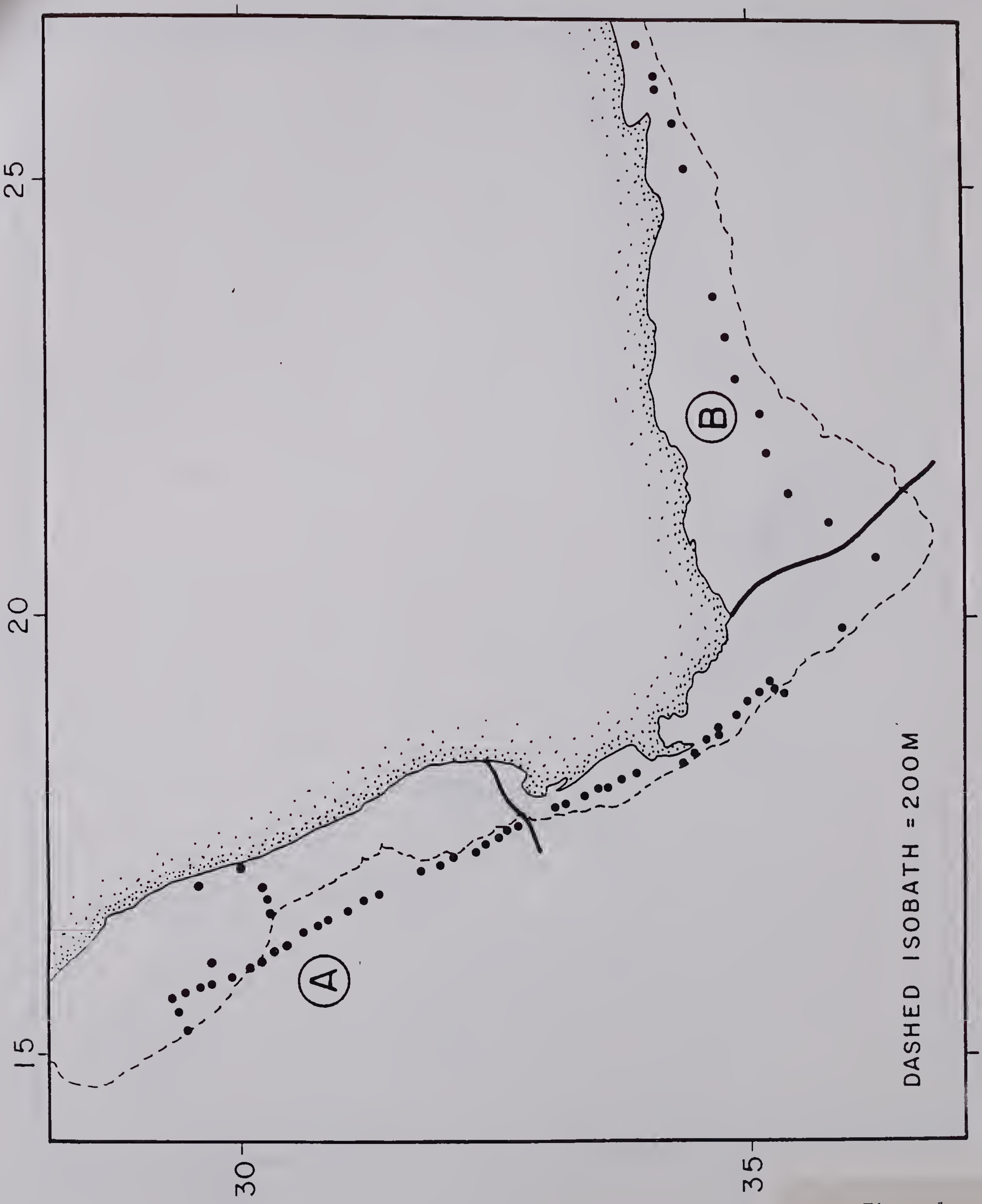

Figure 1a

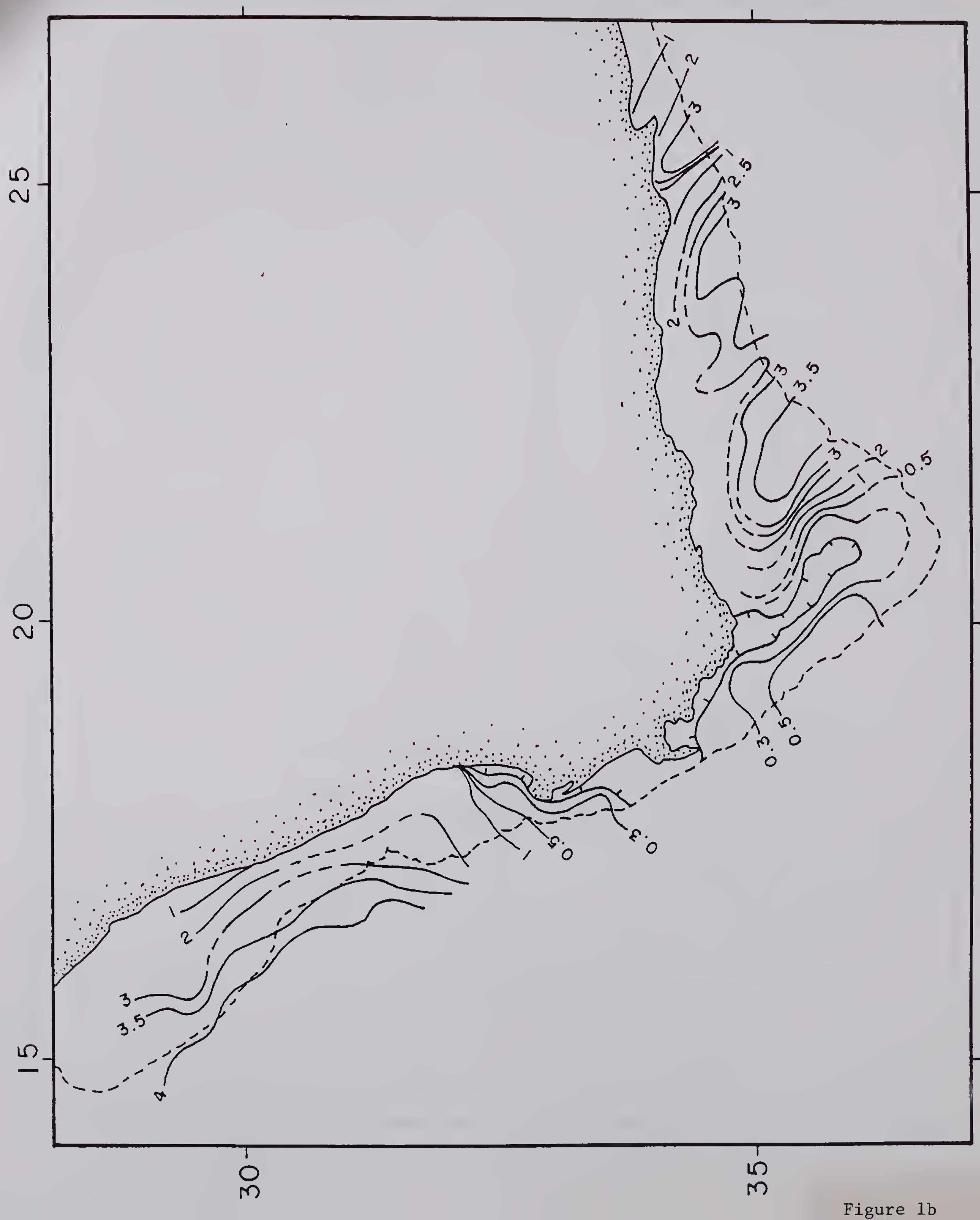

Figure 1b

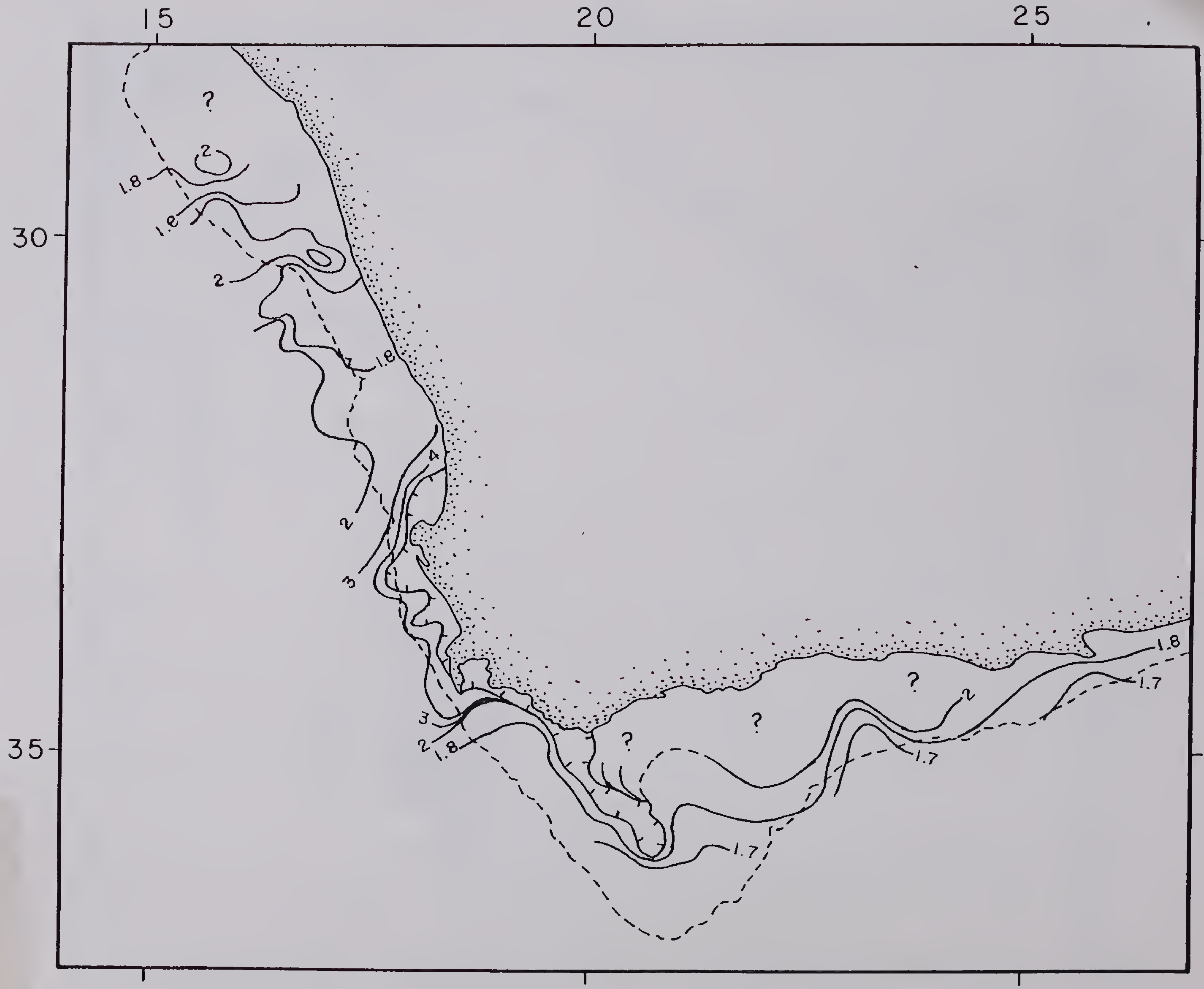

Figure 1c

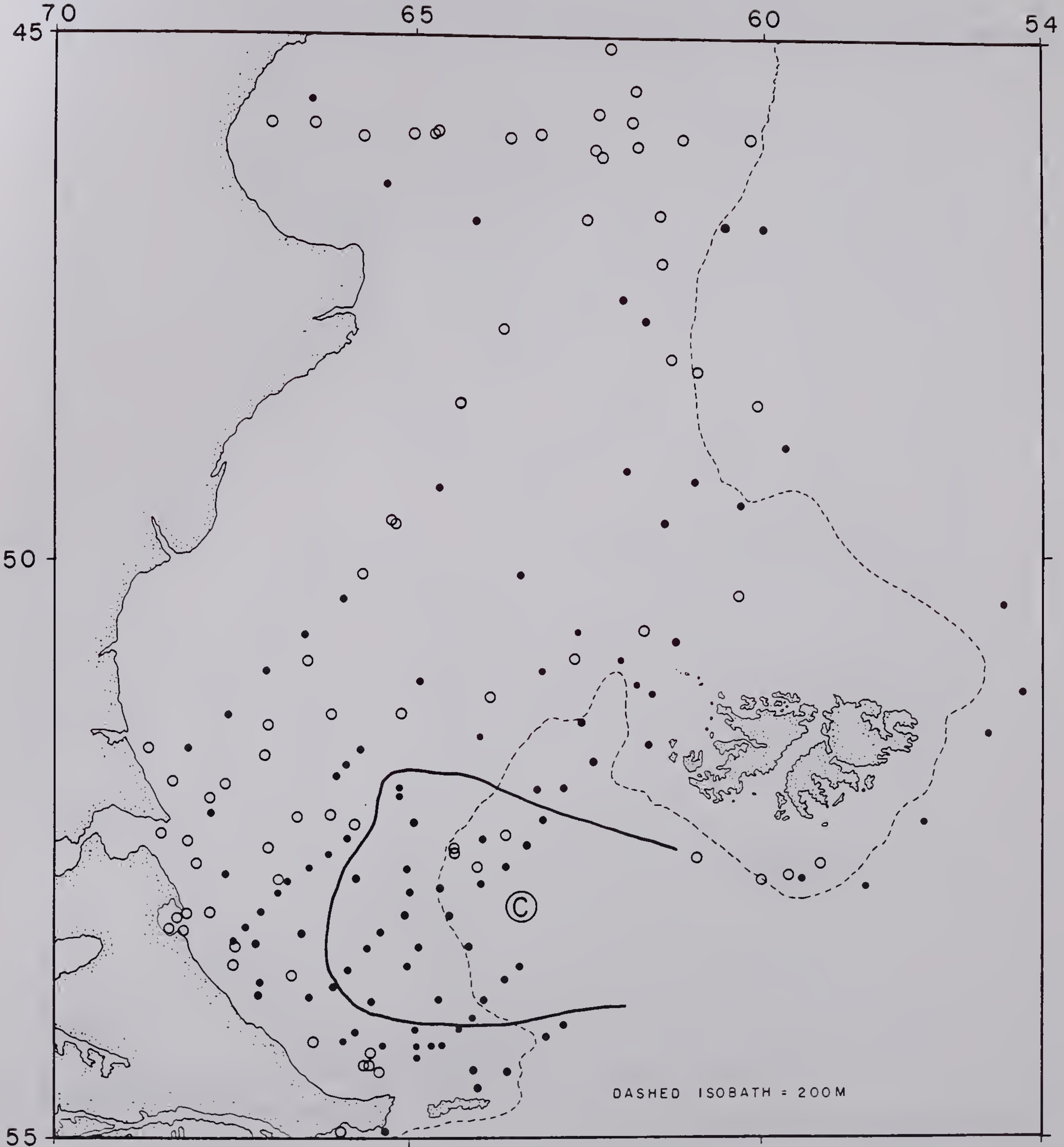

Figure 2a

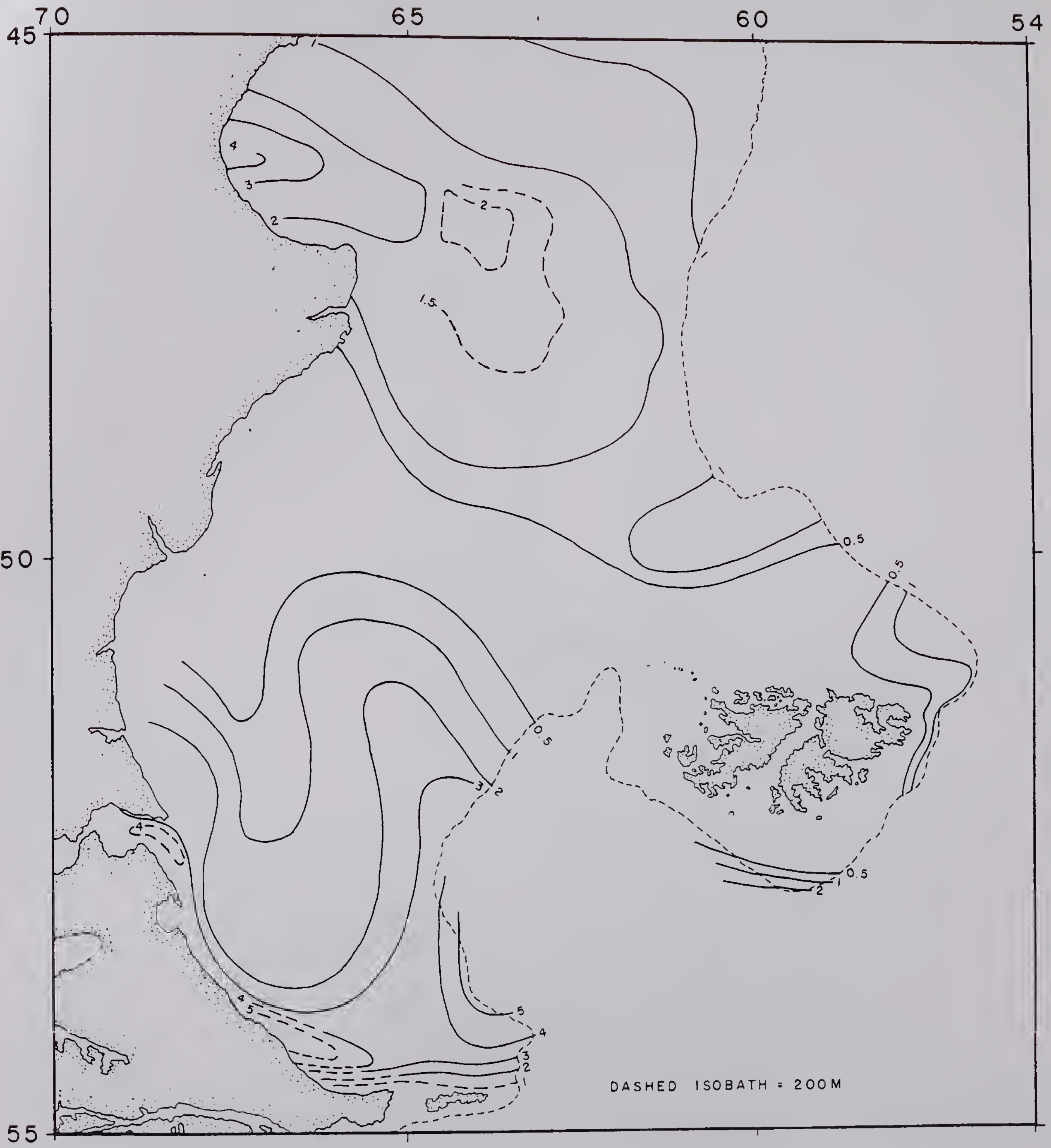
70
65
60
54
45
50
55
4
3
2
2
1.5
0.5
0.5
0.5
3
2
4
0.5
1
2
4
5
5
4
3
2
1
DASHED ISOBATH = 200M

Figure 2b

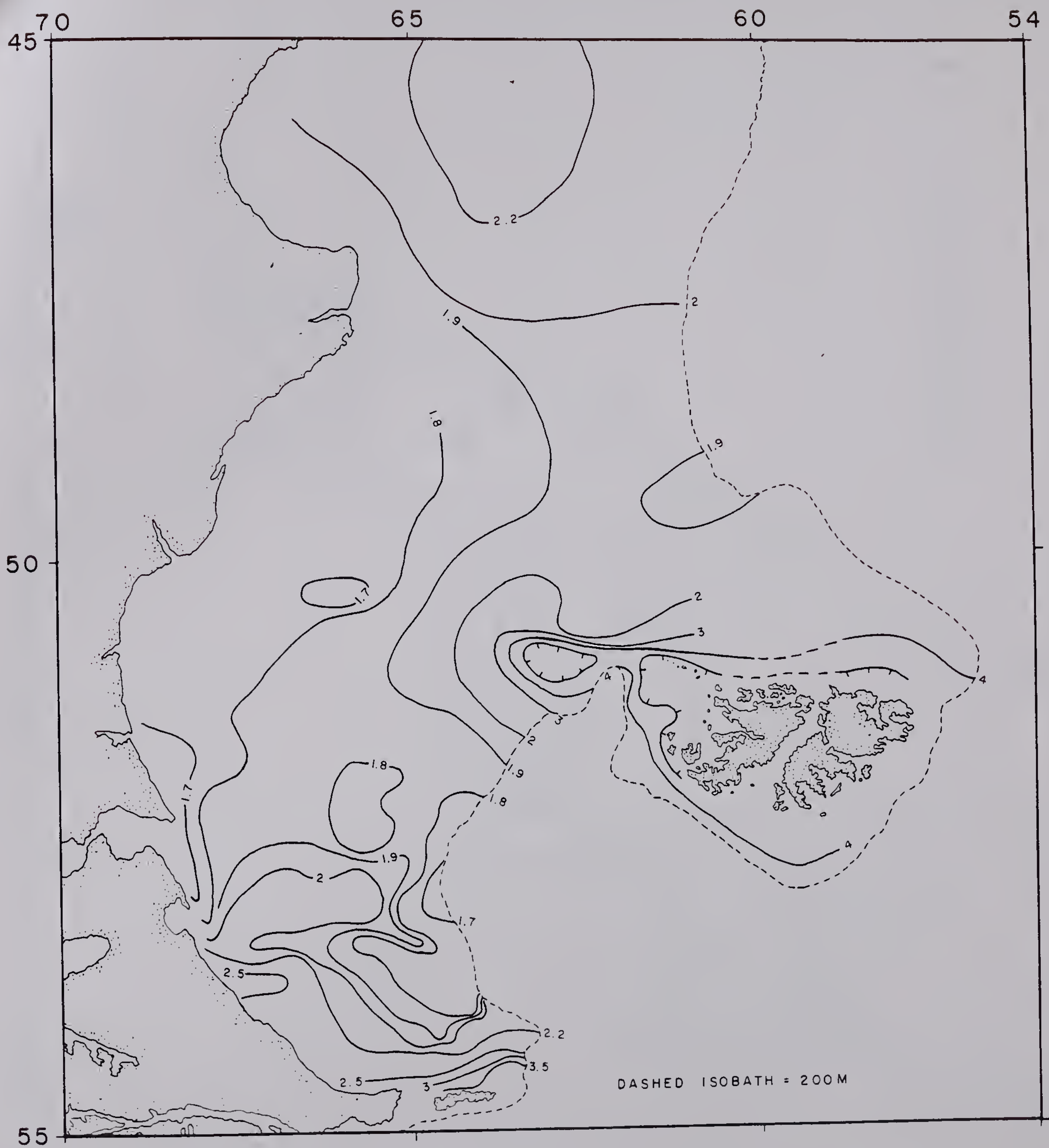
70
65
60
54
45
50
55
2.2
2
1.9
1.8
1.9
1.7
2
3
4
3
2
1.9
1.8
1.8
1.7
1.9
2
1.7
4
2.5
2.2
3.5
2.5
3
DASHED ISOBATH = 200M

Figure 2c

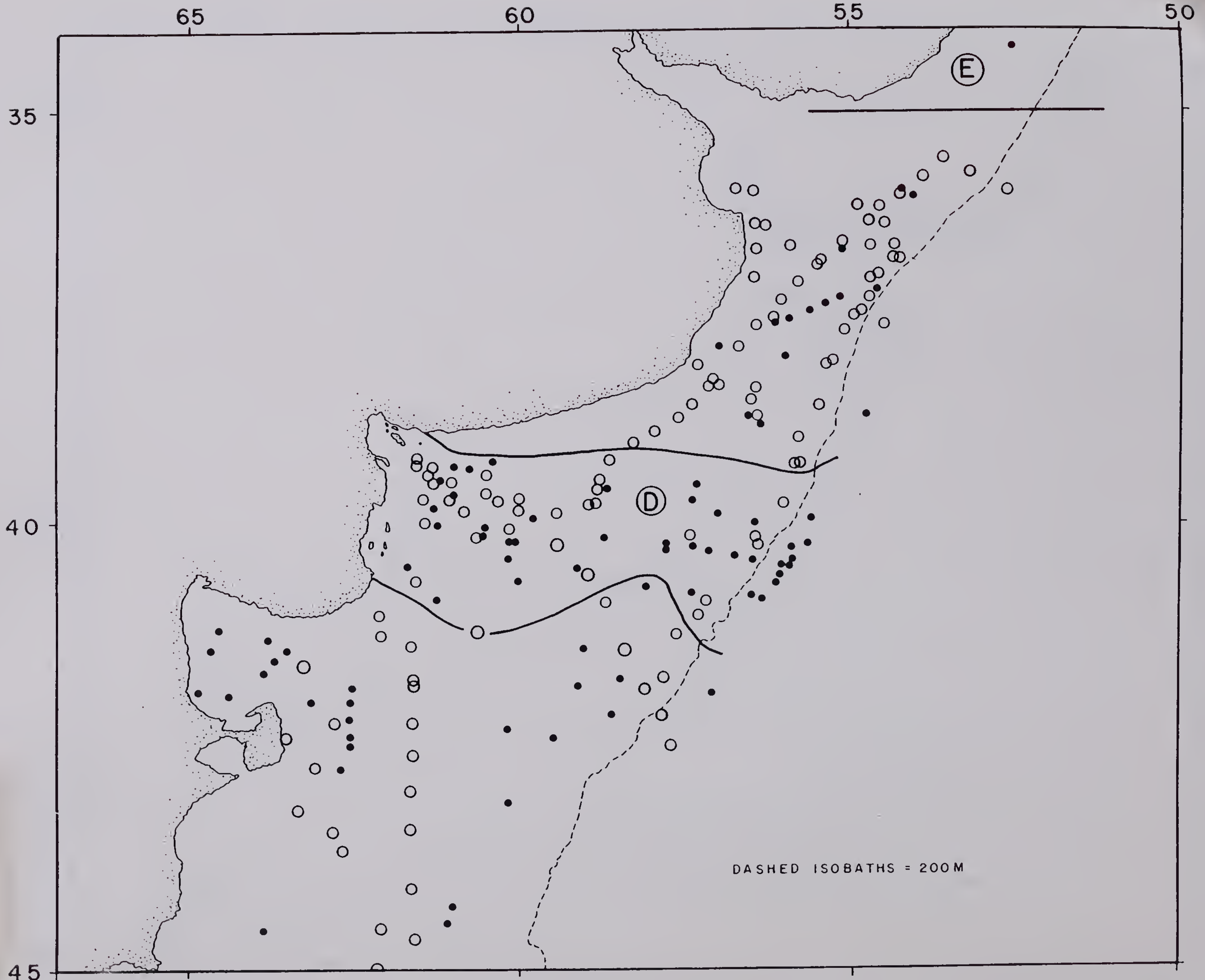

Figure 3a

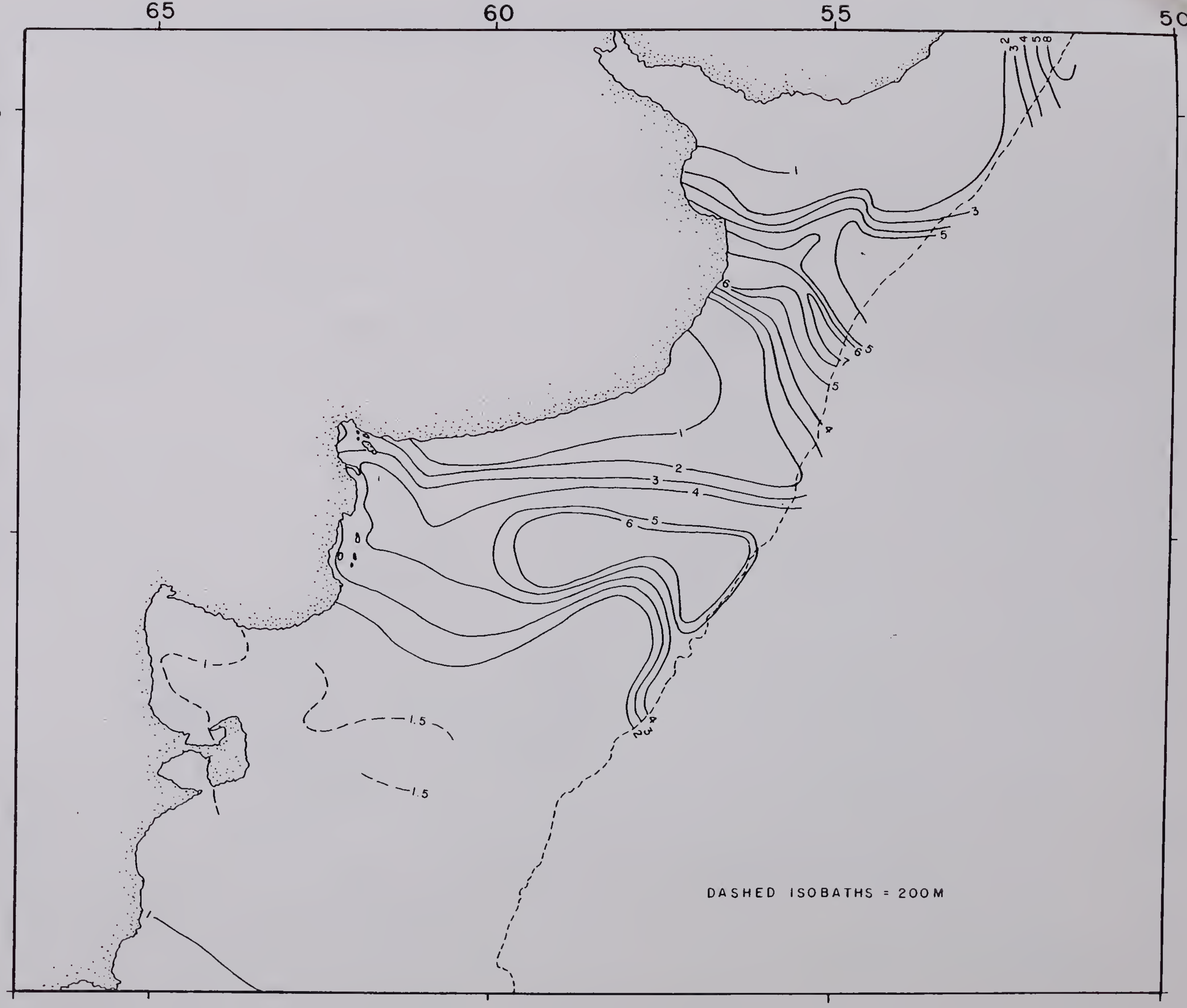

Figure 3b

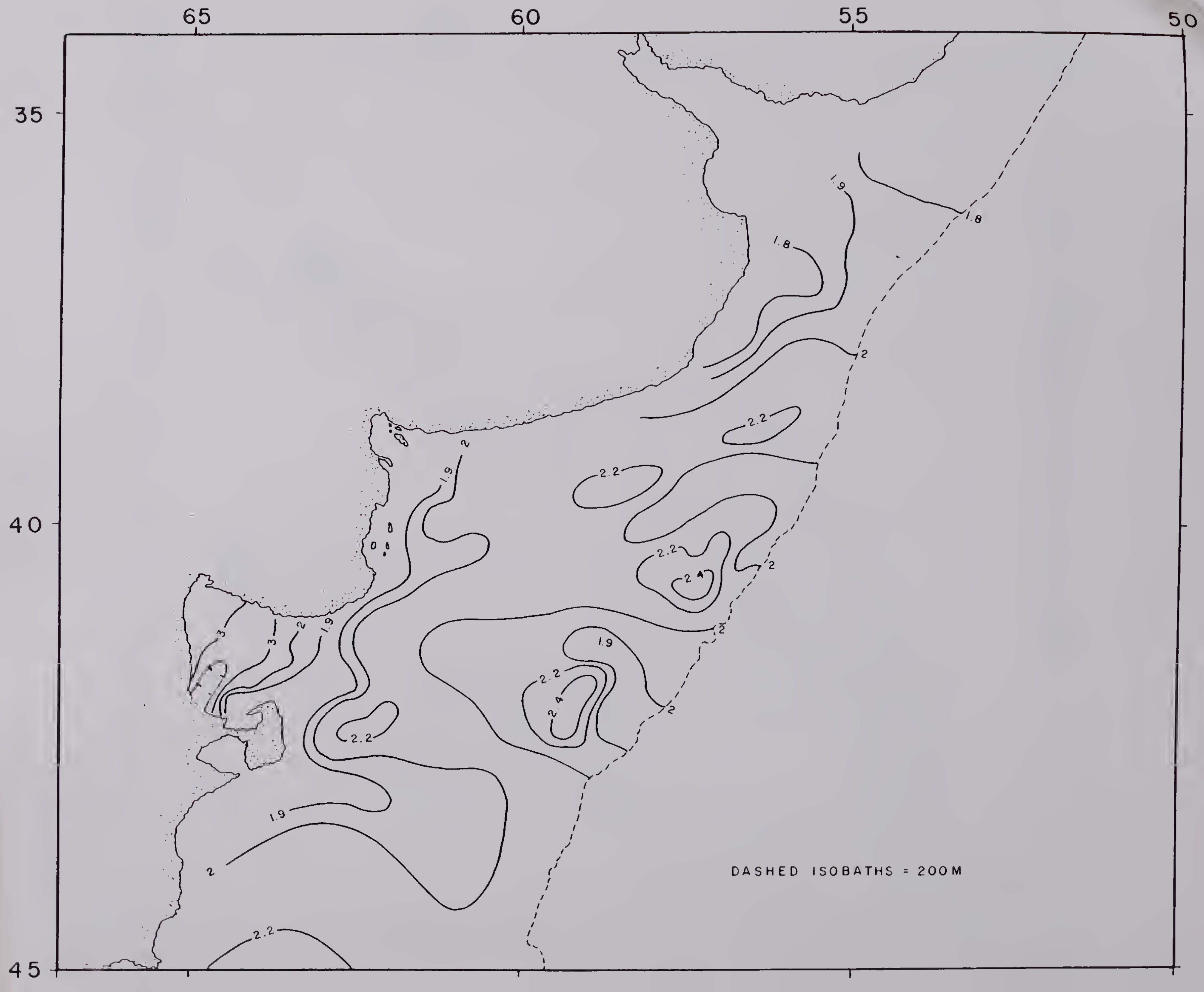
65
60
55
50
35
40
45
1.9
1.8
1.8
2
2.2
2.2
2
2.2
2.4
2
2
1.9
2.2
2.4
2
2
1.9
3
3
2
1.9
2.2
1.9
2
2.2
DASHED ISOBATHS = 200M

Figure 3c

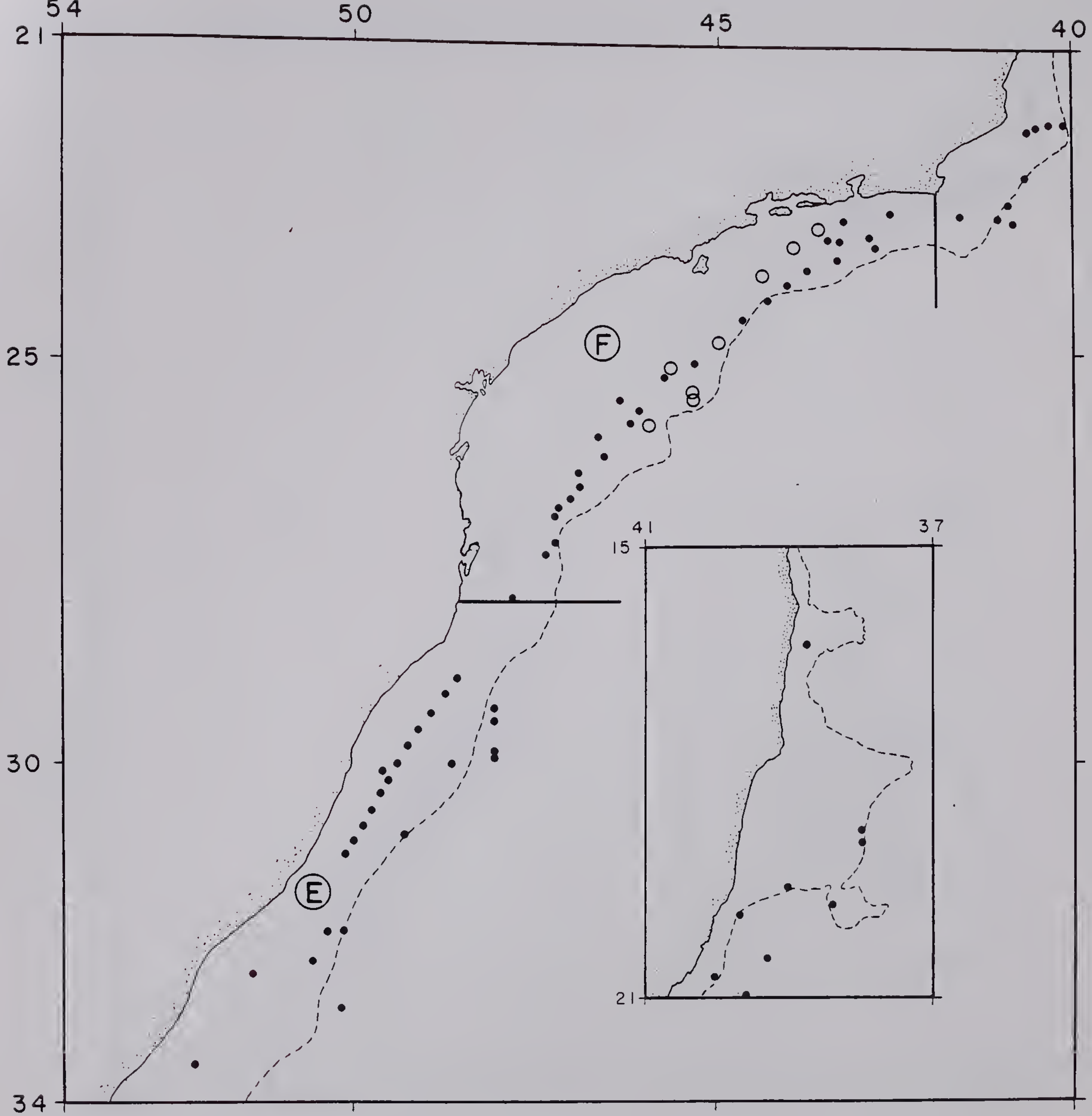

Figure 4a

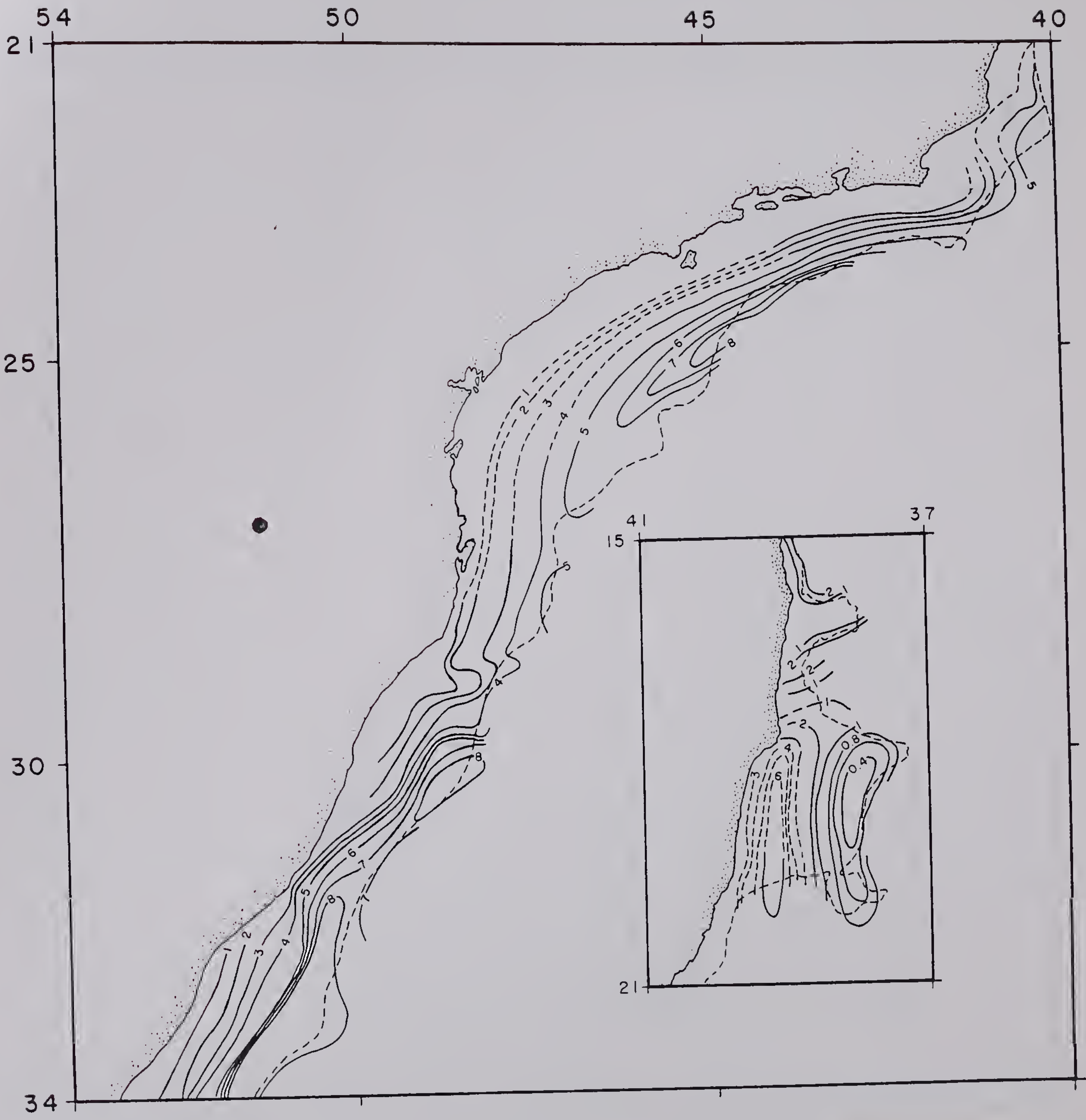

Figure 4b

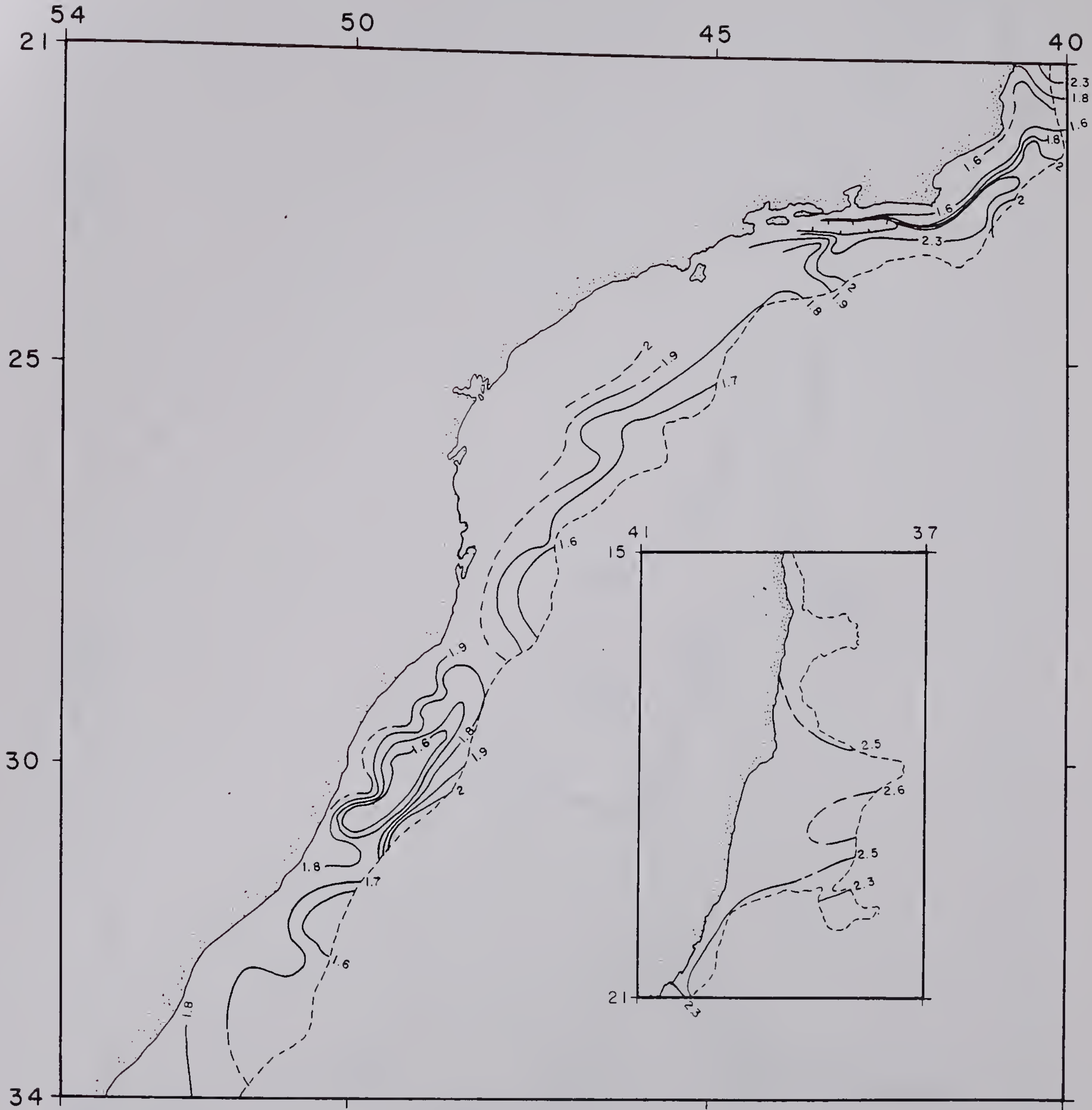
54
50
45
40
21
25
30
34
2.3
1.8
1.6
1.8
2
1.6
2
1.6
2.3
2
1.9
1.8
2
1.9
1.7
1.6
1.9
1.6
1.8
1.9
2
1.8
1.7
1.6
1.8
41
37
15
21
2.5
2.6
2.5
2.3
2.3

Figure 4c

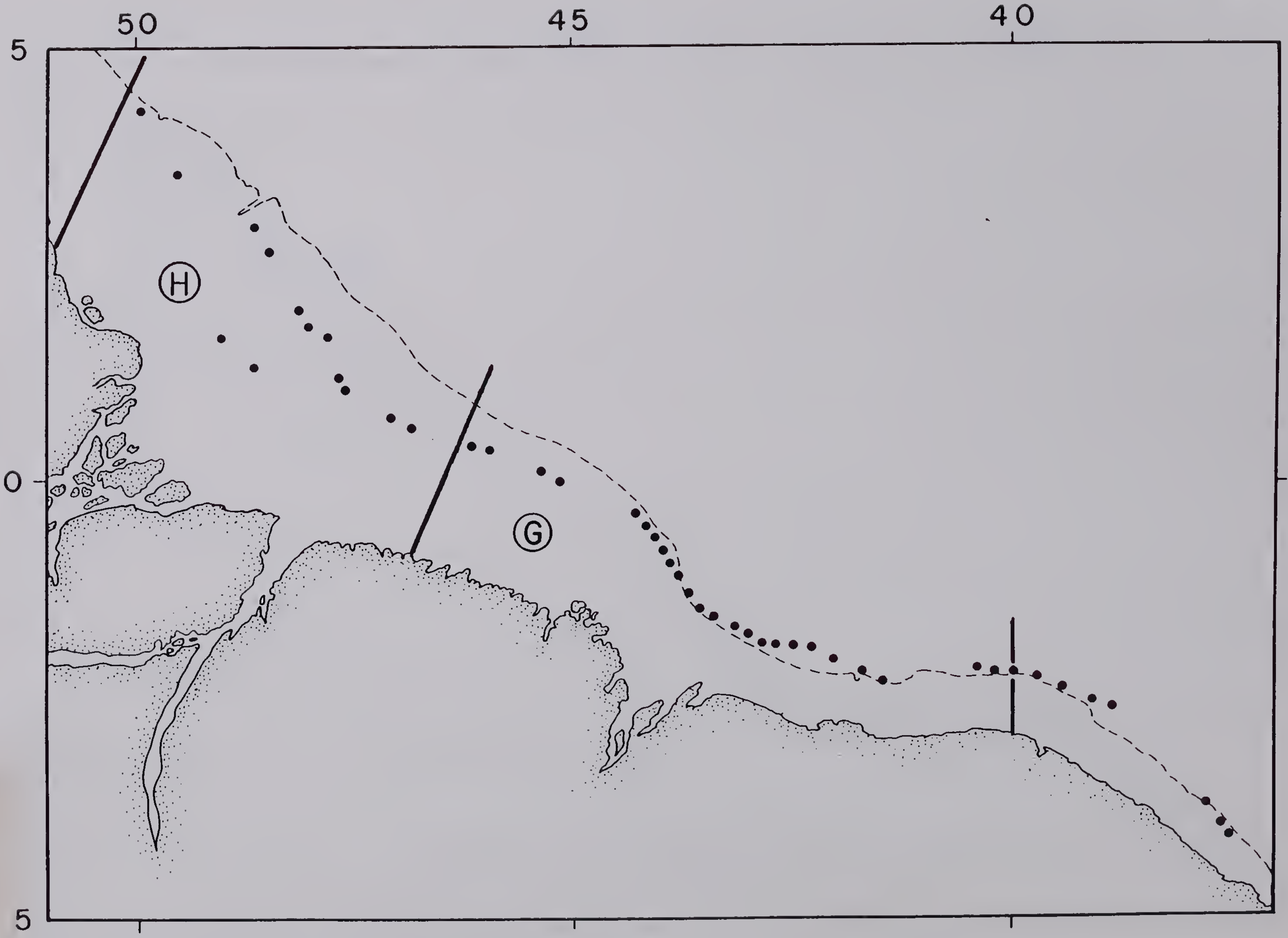

Figure 5a

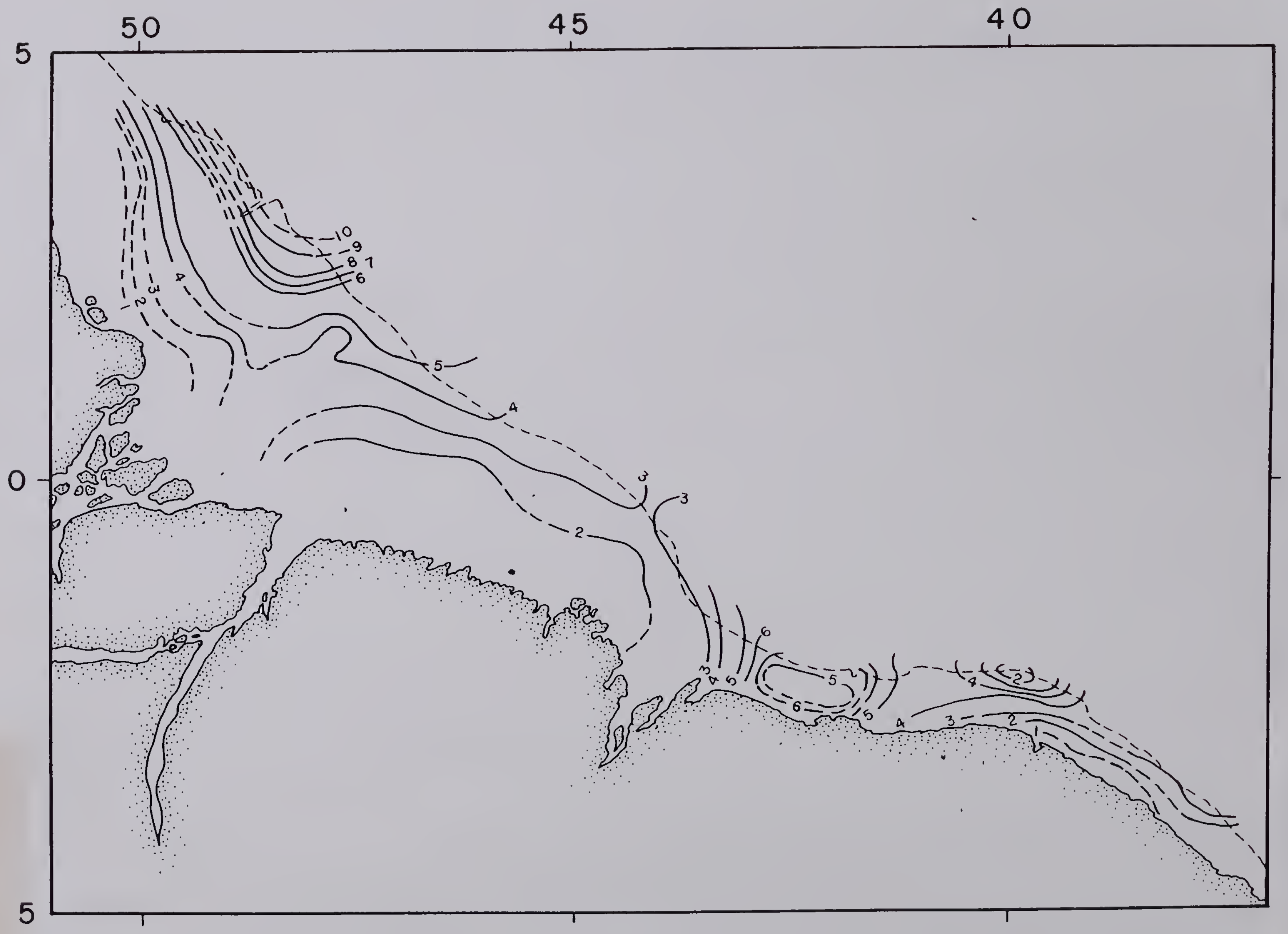

Figure 5b

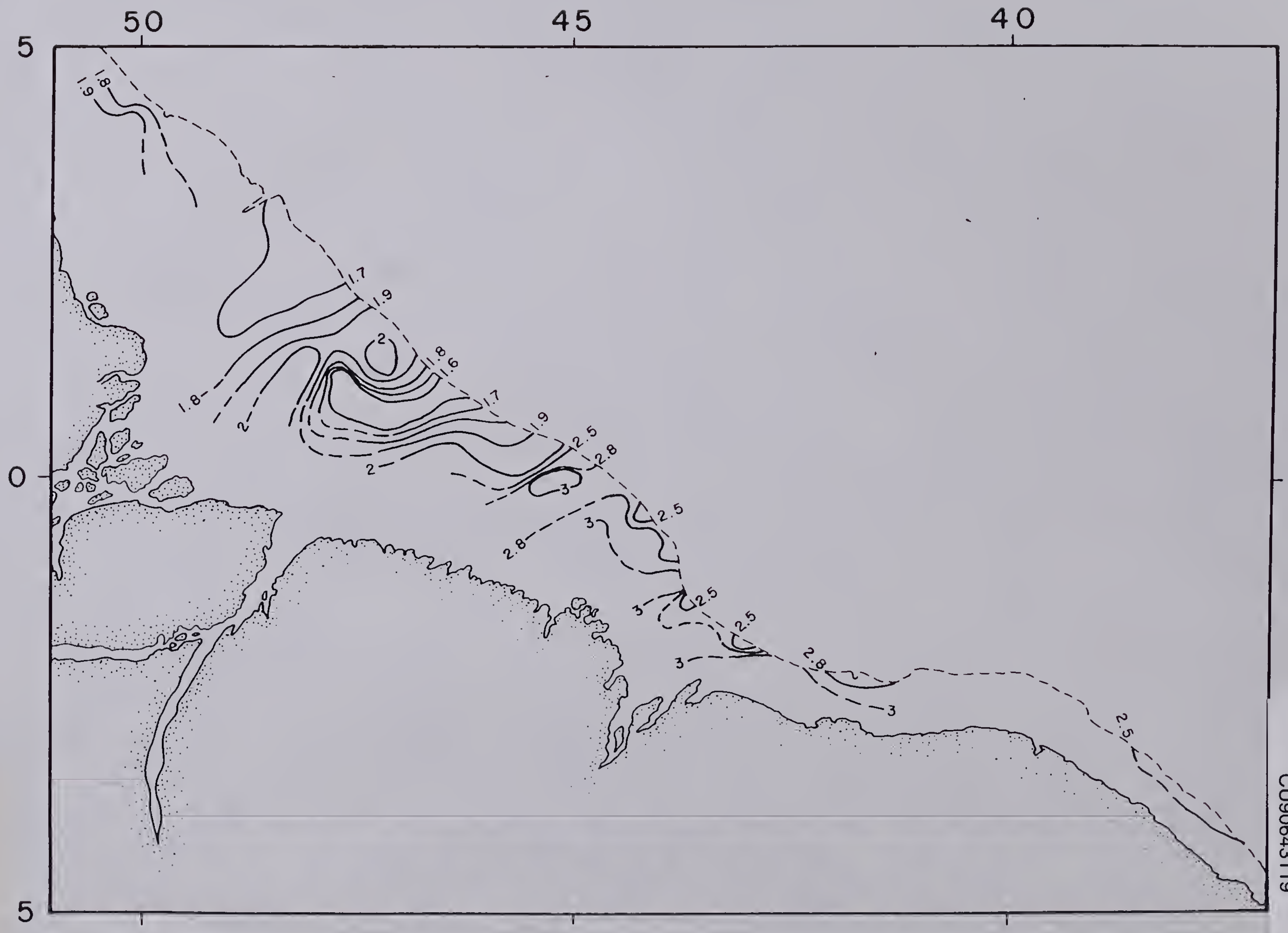
50
45
40
5
0
5
1.9
1.8
1.7
1.9
2
1.8
1.6
1.8
2
1.7
1.9
2.5
2.8
2
3
2.5
3
2.8
2.5
3
2.5
2.8
3
3
2.5

Figure 5c